WARSAW UNIVERSITY OF TECHNOLOGY Index 351733
FACULTY OF CIVIL ENGINEERING
COMMITTEE FOR CIVIL AND WATER ENGINEERING
POLISH ACADEMY OF SCIENCES ISSN 1230-2945

DOI: 10.24425/ace.2021.137173

ARCHIVES OF CIVIL ENGINEERING

Vol. LXVII ISSUE 2 2021

© 2021. S. Czarnecki, T. Lewiński.

s. 355–381

This is an open-access article distributed under the terms of the Creative Commons Attribution-NonCommercial-NoDerivatives License (CC BY-NC-ND 4.0, https://creativecommons.org/licenses/by-nc-nd/4.0/), which per-mits use, distribution, and reproduction in any medium, provided that the Article is properly cited, the use is non-commercial, and no modifications or adaptations are made.

Research paper

Vibrations of bars including transverse shear deformations and warping due to torsion

S. Czarnecki[1], T. Lewiński[2]

Abstract: The paper deals with coupled flexural-torsional vibrations of straight prismatic elastic bars made of a linearly elastic isotropic and homogeneous material. One of the aims is to develop an effective method of modelling vibrations of train rails of cross-sections being mono-symmetric, taking into account warping due to torsion as well as transverse shear deformations. The Librescu-Song 1D model has been appropriately adapted to the above research aims by incorporating all the inertia terms corresponding to the kinematic hypotheses. The finite element(FE) program has been written and its correctness has been verified. The results concerning natural vibrations compare favourably with those predicted by 3D FE modelling using dense meshes. The paper proves that neglecting warping due to torsion leads to omitting several eigen-modes of vibrations, thus showing that the popular Timoshenko-like models are useless for the vibration analysis of bars of mono-symmetric cross sections.

Keywords: theory of bars, coupled flexural-torsional vibrations, Timoshenko theory, Librescu-Song theory

[1] PhD., Eng., Warsaw University of Technology, Faculty of Civil Engineering, Al. Armii Ludowej 16, 00-637 Warsaw, Poland, e-mai: s.czarnecki@il.pw.edu.pl. ORCID: https://orcid.org/0000-0001-9789-7085

[2] Prof., DSc., PhD., Eng., Warsaw University of Technology, Faculty of Civil Engineering, Al. Armii Ludowej 16, 00-637 Warsaw, Poland, e-mail: t.lewiński@il.pw.edu.pl, ORCID: https://orcid.org/0000-0003-2299-2162

1. Introduction

The most advanced 1D theories of elastic bars model their axial deformation, the bending, the non-planar deformations due to transverse shear in two planes as well as the warping due to torsion, while the transverse distortions of the cross sections are neglected, see e.g. El Fatmi [6] and Genoese et al.[7]. By assuming that the non-planar deformations due to transverse shear are characterized by the Timoshenko shear deformation measures and the warping due to torsion is controlled by the conventional measure of torsion, one arrives at the 1D bar model involving the smallest possible number of the primal unknowns: the axial displacement (along the axis x), two transverse displacements (along the axes y and z) , two angles of rotation of the cross section and the angle of axial rotation. In this manner one obtains the simplified theory of El Fatmi equipped with the correct constitutive equations, provided that at least the 1st order approximation warping functions are assumed, see Secs 3, 4 in [11]. By neglecting the out-of-plane deviation of the transverse shear deformation one obtains the model of Librescu and Song, see Sec 3 in [12]. This model extends Timoshenko's theory towards including warping due to torsion. The constitutive equations (along with the stiffnesses) may be still derived from the (more advanced) simplified El Fatmi theory, to make them as accurate as possible; in the present paper these equations are given by (4.3), (4.4). It is worth emphasizing that in these constitutive equations the formulae linking transverse forces with shear deformations are coupled, while all other formulae are decoupled. The mentioned coupling holds even if the cross section parameterization (i.e. the y,z system) refers to the principal axes of inertia. In general, the reciprocal transverse shear stiffnesses $A_{yz} = A_{zy}$ are non- zero, see Eqs. (4.15) in [11]. They vanish if the cross section is mono-symmetric (or bisymmetric). Even if the cross-section is mono-symmetric there are several alternative methods of computing the shear correction factors $k_z = A_z / A$, $k_y = A_y / A$, A being the area of the cross section, see [5,7,8,9]. In the present paper the shear correction factors will be computed according to Gruttmann and Wagner's algorithm [8]; it is more accurate that the algorithm used in [11] where the Poisson ratio effect has been neglected. Nevertheless, the results do not coincide with those predicted by the algorithm of Hutchinson [9], which will be recalled in the context of the elliptic cross-section.

The aim of the present paper is modelling vibrations of prismatic bars of arbitrary cross sections, but the examples will concern the mono-symmetric profiles. The kinematic assumptions will be used like in Librescu-Song's theory, yet the constitutive equations will be assumed as in the simplified El Fatmi's model (because these are the most accurate and also the simplest). The assumed kinematics

admits independence of rotations and deflections; the warping due to torsion is induced by the torsional deformation. This kinematics determines not only the elastic energy of the bar, but also all the inertia terms. The aim of taking into account the terms modelling the torsional warping within the kinematic assumptions is to achieve maximal accuracy of predicting the first, say, 10 natural frequencies. Since the paper by Banerjee [2] appeared it is known that the accurate description of bars' vibration necessitates taking into account the warping effect, especially if the profiles are thin-walled. The essential influence of the warping phenomenon on the dynamical behavior of bars has also been confirmed by Adam [1] and by Bercin and Tanaka [3], where also the shear deformation effect has been included. The history of this development of the theory of vibration of bars can be found in the recent work by Burlon et al [4].

In the present paper the Librescu-Song model is adopted and used to predict natural frequencies of selected bars, including the rail 49E1. This aim is attained by preparing the new FE code in which the primal unknowns are interpolated by 3rd order polynomials. The approach includes solving three elliptic problems posed on the plane cross-section domain, describing the warping due to torsion and shear deformation in two transverse directions. Using the contemporary terminology, the approach is hierarchical: the 3D problem is replaced by three 2D elliptic problems from which some data are transferred to the main problem (posed on the bar's axis) modelling its coupled flexural-torsional vibrations.

The analysis of vibrations of the rail 49E1 is the preliminary study for designing the mass dampers for the rail track; according to the code [13] the supported rail (with dampers) of length 6 m should be tested. This justifies the vibration analysis of the fork-supported rails of the span much longer than the usual distance between the sleepers, see Sec.9.2. Since the rails are subjected to both the vertical and horizontal loads our analysis includes: vertical bending - as well as the coupled: lateral bending-torsional vibrations. This 1D model developed can be appropriately adjusted to analyze vibrations of rail tracks by the methods proposed recently by Kostovasilis et al.[10].

2. Warping due to torsion and transverse shear

Consider first the *warping due to pure torsion*. The warping function will be referred to the shear center S by using Gruttmann and Wagner [8] concept. Let point O be the gravity center of the cross-section's planar domain A, being also the origin of the Cartesian coordinate system (y,z) of axes being the principal axes of the domain A. Let $\Delta = \partial^2/\partial y^2 + \partial^2/\partial z^2$ be the Laplace operator; let $\mathbf{n} = (n_y, n_z)$ be the unit vector outward normal to the contour Γ of the domain A. The directional derivative of the

function f with respect to the vector $\mathbf{n}$ is defined by $\partial f/\partial \mathbf{n} = f_{,y}n_y + f_{,z}n_z$, where $(.)_{,y} = \partial/\partial y$, $(.)_{,z} = \partial/\partial z$. To make the formulae as concise as possible we introduce the notation: $dA=dydz$, $\langle f \rangle = \int_A f(y,z)dA$, $(f\,|\,g) = \int_A f(y,z)g(y,z)dA$. Thus, in particular: $(1\,|\,y)=0$, $(1\,|\,z)=0$, $(y\,|\,z)=0$. The warping function due to pure torsion is determined by the solution $\varpi_o = \varpi_o(y,z)$ to the following elliptic problem posed in the planar domain A:

$$\text{(2.1)} \quad \Delta\varpi_o = 0, \text{ in } A, \quad \frac{\partial \varpi_o}{\partial \mathbf{n}} = n_y z - n_z y \text{ on } \Gamma, \quad \langle \varpi_o \rangle = 0$$

The last condition in (2.1) makes the solution unique. The coordinates of the center of shear S are given by, cf. Gruttmann and Wagner [8]

$$\text{(2.2)} \quad y_S = -\frac{(\varpi_o\,|\,z)}{(z\,|\,z)}, \quad z_S = \frac{(\varpi_o\,|\,y)}{(y\,|\,y)}$$

where $J_y = (z\,|\,z)$, $J_z = (y\,|\,y)$ represent the principal moments of inertia of the cross section domain A. The warping function due to torsion referred to point S is given by

$$\text{(2.3)} \quad \varpi(y,z) = \varpi_o(y,z) + y_S(z - z_S) - z_S(y - y_S),$$

We note that: $(\varpi\,|\,1)=0$, $(\varpi\,|\,y)=0$, $(\varpi\,|\,z)=0$.

Consider now *the effect of the transverse shear*. To make the paper self-contained we recall, yet without explanatory comments, the Gruttmann and Wagner [8] algorithm of computing the shear correction factors of bars made of a homogeneous isotropic material; Poisson's ratio ν and Young's modulus E are material constants. The bar is viewed as prismatic, hence each outward normal to its cylindrical surface is orthogonal to the bar' axis.

Step 1. Computing coordinates of a point S_o

Having the solution to the problem (2.1) we compute

$$\text{(2.4)} \quad B_y = \left((\varpi_{o,z} + y)\,|\,y\right), \; B_z = \left((\varpi_{o,y} - z)\,|\,z\right), \; B_{zz} = \left((\varpi_{o,y} - z)\,|\,z^2\right), B_{yy} = \left((\varpi_{o,z} + y)\,|\,y^2\right)$$

The coordinates of point S_o read $y_o = \dfrac{B_{yy}}{2B_y}$, $z_o = \dfrac{B_{zz}}{2B_z}$.

Step 2. Determination of the stress function modelling the transverse shear in the y-direction. Define

$$\text{(2.5)} \quad f_o^1(y,z) = \frac{1}{J_z}y, \quad f_1(z) = -\frac{\nu}{2(1+\nu)}\frac{(z-z_o)^2}{J_z}$$

and solve the elliptic problem:

(2.6) $\Delta\psi_1 + f_o^1 = 0,\ \text{in } A, \qquad \dfrac{\partial\psi_1}{\partial\mathbf{n}} = f_1(z)\, n_y \text{ on } \Gamma$

The solution is determined up to an additive constant, not important in the sequel.

Step 3 Compute the auxiliary fields $\vartheta_{xy} = \psi_{1,y} - f_1(z),\ \vartheta_{xz} = \psi_{1,z}$ and the integral $W = \left\langle \left(\vartheta_{xy}\right)^2 + \left(\vartheta_{xz}\right)^2 \right\rangle$.The effective area $A_y = k_y A$ is determined by $k_y = (AW)^{-1}$

Step 4. Determination of the stress function modelling the transverse shear in the *z*-direction. Define

(2.7) $f_o^2\left(y,z\right) = \dfrac{1}{J_y} z, \quad f_2\left(y\right) = -\dfrac{\nu}{2(1+\nu)} \dfrac{(y-y_o)^2}{J_y}$

and solve the elliptic problem:

(2.8) $\Delta\psi_2 + f_o^2 = 0,\ \text{in } A, \qquad \dfrac{\partial\psi_2}{\partial\mathbf{n}} = f_2(y)\, n_z \text{ on } \Gamma,$

Step 5 Compute the auxiliary fields $\vartheta_{xy} = \psi_{2,y},\ \vartheta_{xz} = \psi_{2,z} - f_2(y)$ and the integral W defined as above. The effective area $A_z = k_z A$ is determined by $k_z = (AW)^{-1}$.

Having the stress functions ψ_1, ψ_2 and the magnitudes of the transverse forces one can recover the shape of the deformed cross sections, see [8] and the references therein.

3. Kinematic assumptions

As suggested by the theory of pure torsion the variation of the warping due to torsion is determined by the rate of change of the twisting angle. The displacement fields $u_x(x,y,z,t), u_y(x,y,z,t), u_z(x,y,z,t)$ in the bar are assumed to have the form

(3.1)
$$\begin{aligned} &u_x = u(x,t) + y\varphi(x,t) + z\beta(x,t) + \varpi(y,z)\frac{\partial\theta(x,t)}{\partial x}, \\ &u_y = v(x,t) - (z - z_S)\theta(x,t), \quad u_z = w(x,t) + (y - y_S)\theta(x,t), \end{aligned}$$

where $u(x,t), w(x,t), v(x,t), \varphi(x,t), \beta(x,t), \theta(x,t)$ are unknown kinematic fields defined on the *x* axis. We note that *v* and *w* represent displacement of point S along the axes *y* and *z*, respectively. Moreover, $\theta(x,t)$ stands for the infinitesimal angle of rotation around the axis *x*, since: $(u_{z,y} - u_{y,z})/2 = \theta$. Moreover, $u(x) = \langle u_x \rangle / A$, and $\varphi(x) = \left(y \,|\, u_x\right)/J_z,\ \beta(x) = \left(z \,|\, u_x\right)/J_y$; hence $\varphi(x), \beta(x)$ represent the averaged angles of rotation around the axes –*z* and *y*.

Let us define the strain measures of the theory being constructed

$$\varepsilon = \frac{\partial u}{\partial x},\ \ \gamma_z = \beta + \frac{\partial w}{\partial x},\ \ \kappa_y = \frac{\partial \beta}{\partial x},\ \ \gamma_y = \varphi + \frac{\partial v}{\partial x},\ \ \kappa_z = -\frac{\partial \varphi}{\partial x},\ \ \rho = \frac{\partial \theta}{\partial x},\ \ \kappa_\varpi = \frac{\partial^2 \theta}{\partial x^2}. \tag{3.2}$$

The strain ε represents the axial deformation, γ_z, γ_y represent measures of transverse shear, κ_y, κ_z stand for the measures of bending; ρ is the measure of torsion; κ_ϖ describes the warping due to torsion, like in Vlasov's theory of bars, see [11]. The time-independent virtual displacement fields $\bar{u}(x), \bar{w}(x), \bar{v}(x), \bar{\varphi}(x), \bar{\beta}(x), \bar{\theta}(x)$ determine the virtual strain measures by the same rules (3.2); only then the partial derivatives are replaced by ordinary derivatives with respect to x. The kinematic assumptions (3.1) lead to the following formulae for the strain components

$$\begin{aligned} &\varepsilon_x = \varepsilon - y\kappa_z + z\kappa_y + \varpi(y,z)\kappa_\varpi,\ \ \varepsilon_y = 0,\ \ \varepsilon_z = 0, \\ &\gamma_{xy} = \left(\varpi_{,y} - z + z_S\right)\rho + \gamma_y,\ \ \gamma_{xz} = \left(\varpi_{,z} + y - y_S\right)\rho + \gamma_z,\ \ \gamma_{yz} = 0 \end{aligned} \tag{3.3}$$

The virtual strains are expressed the same way.

4. Stress resultants and constitutive equations

The virtual work of stresses, or the integral of the expression

$$(\sigma_x \bar{\varepsilon}_x + \sigma_y \bar{\varepsilon}_y + \sigma_z \bar{\varepsilon}_z + \tau_{xy}\bar{\gamma}_{xy} + \tau_{xz}\bar{\gamma}_{xz} + \tau_{zy}\bar{\gamma}_{zy})$$

over the bar domain assumes the form compatible with (3.3)

$$\bar{L}_{\text{int}} = \int_0^l \left(N\bar{\varepsilon} + T_z\bar{\gamma}_z + M_y\bar{\kappa}_y + T_y\bar{\gamma}_y + M_z\bar{\kappa}_z + \mathcal{M}\bar{\rho} + B\bar{\kappa}_\varpi \right) dx \tag{4.1}$$

where the stress resultants are given by

$$\begin{aligned} &N = \langle \sigma_x \rangle,\ T_z = \langle \tau_{xz} \rangle,\ \ T_y = \langle \tau_{xy} \rangle, M_y = (z \mid \sigma_x),\ \ ,\ \ M_z = -(y \mid \sigma_x), \\ &\mathcal{M} = \left((\varpi_{,z} + y - y_S) \mid \tau_{xz} \right) + \left((\varpi_{,y} - z + z_S) \mid \tau_{xy} \right),\ B = (\varpi \mid \sigma_x) \end{aligned} \tag{4.2}$$

We recognize the well-known internal forces: the axial force N, the transverse forces T_z, T_y, the bending moments M_y, M_z, the torsional moment $\mathcal{M}$ and the bimoment B, defined similarly as in Vlasov's theory. Only now the definitions (4.2) refer to bars of arbitrary cross sections; in particular, the bimoment is expressed by the surface integral, without any reference to the sectional coordinate parameterization. The constitutive equations of the material of the bar are assumed in the form usually used while constructing the theory of thin bars: $\sigma_x = E\varepsilon_x$, $\tau_{xy} = G\gamma_{xy}$, $\tau_{xz} = G\gamma_{xz}$, where

$E = 2\,(1+\nu)\,G$, G being the shear modulus. The constitutive equations of the 1D bar model turn out to have the form, see [11]

(4.3) $N = EA\varepsilon,\ B = EJ_{\varpi}\kappa_{\varpi},\ M_y = EJ_y\kappa_y,\ \ M_z = EJ_z\kappa_z$

(4.4) $T_z = GA_z\gamma_z + GA_{zy}\gamma_y,\ \ T_y = GA_{yz}\gamma_z + GA_y\gamma_y\ \ \mathcal{M} = GJ\rho$

where

(4.5) $J_{\varpi} = \left(\varpi \,|\, \varpi\right),\quad J = \left\langle (\varpi_{,y} - z + z_S)^2 + (\varpi_{,z} + y - y_S)^2 \right\rangle$

and $A_z = k_z A,\ A_{zy} = A_{yz} = k_{zy}A,\ A_y = k_y A$. The shear correction factors can be determined in various manners, see [5,7,8,9]. In case of mono-symmetric (hence also -bisymmetric) cross sections $k_{zy} = 0$ and the remaining shear correction factors k_z, k_y can be computed by the algorithm recalled in Sec. 2 of the present paper.

5. Virtual work of loads and inertia forces

The load applied to the surface of the cylindrical domain of the prismatic bar considered does the virtual work which can be expressed as the line integral

(5.1) $\bar{L}_{span} = \int_0^l \left(p\bar{u} + q_z\bar{w} + q_y\bar{v} + m_s\bar{\theta} \right) dx$

here $p(x,t)$ represents the intensity of the axial load reduced to the axis x; $q_z(x,t), q_y(x,t)$ stand for the intensities of the transverse loads reduced to the bar's axis; $m_s(x,t)$ is the intensity of the torsional load. The bending loads are omitted, as usually accepted in case of thin bars.

Assume that the section x=0 is clamped and the end x=l is free, loaded by the tractions of intensities $t_x(y,z),\ t_y(y,z),\ t_z(y,z)$. The virtual work of the tractions is given by:

(5.2) $\bar{L}_{ends} = \int_A \left(t_x\bar{u}_x + t_y\bar{u}_y + t_z\bar{u}_z \right) dA$

Substitution of the kinematic assumptions (3.1) rearranges this virtual work to the form

(5.3) $\bar{L}_{ends} = \tilde{N}\bar{u}(l) + \tilde{M}_y\bar{\beta}(l) + \tilde{T}_z\bar{w}(l) + \tilde{\mathcal{M}}\bar{\theta}(l) + \tilde{B}\dfrac{d\bar{\theta}}{dx}(l) + \tilde{M}_z(-\bar{\varphi}(l)) + \tilde{T}_y\bar{v}(l)$,

the end-forces and end-moments at x=l being given by

$$\tilde{N}(t)=\langle t_x\rangle,\ \tilde{M}_y(t)=(z\,|\,t_x),\ \tilde{T}_z(t)=\langle t_z\rangle,\ \tilde{M}_z(t)=-(y\,|\,t_x),\ \tilde{T}_y(t)=\langle t_y\rangle,$$
$$\tilde{\mathcal{M}}(t)=((y-y_S)\,|\,t_z)-((z-z_S)\,|\,t_y),\ \tilde{B}(t)=(\varpi\,|\,t_x) \tag{5.4}$$

Let $\rho_m(x,y,z)$ be the mass density. The virtual work of the inertia forces is

$$\bar{L}_{inertia}=-\int_0^l\int_A \rho_m\left(\ddot{u}_x\bar{u}_x+\ddot{u}_y\bar{u}_y+\ddot{u}_z\bar{u}_z\right)dAdx \tag{5.5}$$

where the dot "." implies differentiation in time. Let us introduce the inertial characteristics

$$\mu=\langle\rho_m\rangle,\ \mu_\varpi=\left(\varpi^2\,|\,\rho_m\right),\ I_y=\left((z-z_S)^2\,|\,\rho_m\right),\ I_z=\left((y-y_S)^2\,|\,\rho_m\right)$$
$$I_o=I_y+I_z,\ I_{yz}=\left(yz\,|\,\rho_m\right),\ \tilde{I}_y=\left((z^2\,|\,\rho_m\right),\ \tilde{I}_z=\left(y^2\,|\,\rho_m\right), \tag{5.6}$$
$$\hat{S}_y=\left((z-z_S)\,|\,\rho_m\right),\ \hat{S}_z=\left((y-y_S)\,|\,\rho_m\right)$$

Imposing the kinematic constraints (3.1)-without any corrections-gives

$$\bar{L}_{inertia}=-\int_0^l[\Psi_x\bar{u}+\Psi_y\bar{v}+\Psi_z\bar{w}+\Phi_x\bar{\theta}+\Phi_y\bar{\beta}+\Phi_z\bar{\varphi}+\Psi_\varpi\frac{d\bar{\theta}}{dx}]dx\,. \tag{5.7}$$

The inertia forces involved in (5.7) are given by

$$\Psi_x=\mu\ddot{u},\ \ [\Phi_y\Psi_z\Phi_z\Psi_y\Phi_x]^T=\mathbf{S}\ddot{\mathbf{q}},\ \ \Psi_\varpi=\mu_\varpi\frac{\partial\ddot{\theta}}{\partial x} \tag{5.8}$$

where $\mathbf{q}=[\beta\ w\ \varphi\ v\ \theta]^T$ and

$$\mathbf{S}=\begin{bmatrix}\tilde{I}_y & 0 & I_{yz} & 0 & 0\\ 0 & \mu & 0 & 0 & \hat{S}_z\\ I_{yz} & 0 & \tilde{I}_z & 0 & 0\\ 0 & 0 & 0 & \mu & -\hat{S}_y\\ 0 & \hat{S}_z & 0 & -\hat{S}_y & I_o\end{bmatrix}. \tag{5.9}$$

6. Equations of motion and boundary conditions

The motion is governed by the variational equation

$$\bar{L}_{\text{int}}=\bar{L}_{span}+\bar{L}_{ends}+\bar{L}_{inertia}\quad\text{for each } \bar{u},\bar{w},\bar{v},\bar{\beta},\bar{\varphi},\bar{\theta}\text{ kinematically admissible}\,. \tag{6.1}$$

By making use of arbitrariness of the virtual fields we obtain

$$
\begin{aligned}
&\int_0^l N\bar{\varepsilon}dx = \int_0^l (p-\Psi_x)\bar{u}dx + \tilde{N}\bar{u}(l) \\
(6.2)\quad &\int_0^l (M_y\bar{\kappa}_y + T_z\bar{\gamma}_z)dx = \int_0^l [(q_z-\Psi_z)\bar{w} - \Phi_y\bar{\beta}]dx + \tilde{T}_z\bar{w}(l) + \tilde{M}_y\bar{\beta}(l) \\
&\int_0^l (M_z\bar{\kappa}_z + T_y\bar{\gamma}_y)dx = \int_0^l [(q_y-\Psi_y)\bar{v} - \Phi_z\bar{\varphi}]dx + \tilde{T}_y\bar{v}(l) + \tilde{M}_z(-\bar{\varphi}(l)) \\
&\int_0^l \left(B\bar{\kappa}_\varpi + \mathcal{M}\bar{\rho}\right)dx = \int_0^l [(m_s-\Phi_x)\bar{\theta} - \Psi_\varpi \frac{d\bar{\theta}}{dx}]dx + \tilde{B}\frac{d\bar{\theta}}{dx}(l) + \tilde{\mathcal{M}}\bar{\theta}(l)
\end{aligned}
$$

for each $\bar{u}, \bar{w}, \bar{\beta}, \bar{v}, \bar{\varphi}, \bar{\theta}$ kinematically admissible. Localization of the above equations leads to the differential equations of motion

$$
\begin{aligned}
(6.3)\quad &-\frac{\partial N}{\partial x} + \Psi_x = p, \quad -\frac{\partial M_y}{\partial x} + T_z + \Phi_y = 0, \quad -\frac{\partial T_z}{\partial x} + \Psi_z = q_z, \quad \frac{\partial M_z}{\partial x} + T_y + \Phi_z = 0, \\
&-\frac{\partial T_y}{\partial x} + \Psi_y = q_y, \quad -\frac{\partial \mathcal{M}^{eff}}{\partial x} + \Phi_x = m_s, \quad \mathcal{M}^{eff} = \mathcal{M} - \frac{\partial B}{\partial x} + \Psi_\varpi
\end{aligned}
$$

and - to the natural boundary conditions at the free end:

$$
\begin{aligned}
(6.4)\quad &N(l,t) = \tilde{N}(t),\ B(l,t) = \tilde{B}(t),\ M_y(l,t) = \tilde{M}_y(t), \\
&T_z(l,t) = \tilde{T}_z(t),\ M_z(l,t) = \tilde{M}_z(t),\ T_y(l,t) = \tilde{T}_y(t),\ \mathcal{M}^{eff}(l,t) = \tilde{\mathcal{M}}(t)
\end{aligned}
$$

The problem of axial deformation can be solved independently. The other equations are coupled due to the presence of inertia terms. The theory admits the boundary conditions concerning:

N or u, M_y or β, T_z or w, B or $\frac{\partial\theta}{\partial x}$, M_z or $-\varphi$, T_y or v $\mathcal{M}^{eff}$ or θ

hence 2^7 types of the boundary conditions are possible. Among them the fork support means that the quantities: N, M_y, w, B, M_z, v, θ are prescribed. The theory of vibrating bars is now constructed; it will be called the Librescu-Song model.

Assume that the bar is prismatic. By substituting (4.3), (4.4) into (6.3) and taking into account the strain definitions (3.2) one arrives at the equations of motion expressed in terms of the fields: u and $\mathbf{q} = [\beta\ w\ \varphi\ v\ \theta]^T$:

$$
(6.5)\qquad -EA\frac{\partial^2 u}{\partial x^2} + \mu\ddot{u} = 0, \qquad \left(\mathbf{L} + (\mathbf{S}-\mathbf{C})\frac{\partial^2}{\partial t^2}\right)\mathbf{q} + \mathbf{Q} = \mathbf{0}
$$

where $\mathbf{Q}=[0\ q_z\ 0\ q_y\ m_s]^T$ and : $\mathbf{L}=[L_{ij}]_{i,j=1,\ldots,5}$, $\mathbf{C}=\left[C_{ij}\right]_{i,j=1,\ldots,5}$, are the matrices of differential operators defined by

$$C_{ij}=\delta_{i5}\delta_{j5}\mu_{\varpi}\frac{\partial^2}{\partial x^2} \tag{6.6}$$

and

$$\mathbf{L}=\begin{bmatrix} -EJ_y\dfrac{\partial^2}{\partial x^2}+GA_z & GA_z\dfrac{\partial}{\partial x} & GA_{yz} & GA_{yz}\dfrac{\partial}{\partial x} & 0 \\ -GA_z\dfrac{\partial}{\partial x} & -GA_z\dfrac{\partial^2}{\partial x^2} & -GA_{yz}\dfrac{\partial}{\partial x} & -GA_{yz}\dfrac{\partial^2}{\partial x^2} & 0 \\ GA_{yz} & GA_{yz}\dfrac{\partial}{\partial x} & -EJ_z\dfrac{\partial^2}{\partial x^2}+GA_y & GA_y\dfrac{\partial}{\partial x} & 0 \\ -GA_{yz}\dfrac{\partial}{\partial x} & -GA_{yz}\dfrac{\partial^2}{\partial x^2} & -GA_y\dfrac{\partial}{\partial x} & -GA_y\dfrac{\partial^2}{\partial x^2} & 0 \\ 0 & 0 & 0 & 0 & EJ_{\varpi}\dfrac{\partial^4}{\partial x^4}-GJ\dfrac{\partial^2}{\partial x^2} \end{bmatrix} \tag{6.7}$$

The equations $(6.5)_2$ are coupled. In case of ρ_m being constant we have:

$$\begin{aligned} &I_{yz}=0,\quad \hat{S}_y=-z_S\rho_m A,\ \hat{S}_z=-y_S\rho_m A,\ \mu=\rho_m A,\quad \mu_{\varpi}=\rho_m J_{\varpi} \\ &\tilde{I}_y=\rho_m J_y,\ \tilde{I}_z=\rho_m J_z,\ I_y=\rho_m\left[J_y+(z_S)^2A\right],\ I_z=\rho_m\left[J_z+(y_S)^2A\right] \end{aligned} \tag{6.8}$$

the equations being still coupled.

Case of mono-symmetric profiles. If additionally the y=0 axis is the axis of symmetry of the domain A then

$$\begin{aligned} &y_S=0,\ A_{yz}=0,\ I_{yz}=0,\quad \hat{S}_y=-z_S\rho_m A,\ \hat{S}_z=0 \\ &\tilde{I}_y=\rho_m J_y,\ \tilde{I}_z=\rho_m J_z,\quad \mu=\rho_m A,\quad \mu_{\varpi}=\rho_m J_{\varpi} \\ &I_y=\rho_m\left[J_y+(z_S)^2A\right],\ I_z=\tilde{I}_z,\quad I_o=\rho_m\left[J_y+J_z+(z_S)^2A\right] \end{aligned} \tag{6.9}$$

The matrix **S** and the matrix **L** of the differential operators assume block forms. The governing equations $(6.5)_2$ split up into:

a) equations involving $[\beta\ w\ ]^T$ as unknowns; they model the transverse vibrations in the *x-z* plane:

$$\left(-EJ_y\frac{\partial^2}{\partial x^2}+GA_z\right)\beta+GA_z\frac{\partial w}{\partial x}+\tilde{I}_y\ddot{\beta}=0$$
$$-GA_z\frac{\partial\beta}{\partial x}-GA_z\frac{\partial^2 w}{\partial x^2}+\mu\ddot{w}=q_z \tag{6.10}$$

b) equations involving $[\varphi\ v\ \theta]^T$; they model the lateral (or- in the *x-y* plane) bending-torsional vibrations:

$$\left(-EJ_z\frac{\partial^2}{\partial x^2}+GA_y\right)\varphi+GA_y\frac{\partial v}{\partial x}+\tilde{I}_z\ddot{\varphi}=0$$
$$-GA_y\frac{\partial\varphi}{\partial x}-GA_y\frac{\partial^2 v}{\partial x^2}+\mu\ddot{v}-\hat{S}_y\ddot{\theta}=q_y \tag{6.11}$$
$$\left(EJ_\varpi\frac{\partial^4}{\partial x^4}-GJ\frac{\partial^2}{\partial x^2}\right)\theta-\mu_\varpi\frac{\partial^2\ddot{\theta}}{\partial x^2}-\hat{S}_y\ddot{v}+I_o\ddot{\theta}=m_s$$

We see that the rotary inertia $\hat{S}_y$ couples the torsion with the lateral bending. This inertia vanishes only if the points S and O coincide, or if the profile is bisymmetric. Then the torsional vibration becomes an independent phenomenon, unless the kinematic boundary conditions couple twisting with bending.

Remark

The equations (6.11) coincide with those considered in Bercin and Tanaka[3], upon replacing $v,\varphi,\theta,\mu,\hat{S}_y,\ I_o,J_\varpi,J,J_z,A_y,\tilde{I}_z,\mu_\varpi$ by $v,-\theta,\phi,m,em,\ I_s,\Gamma,J,I,kA,J_c,0$, respectively.

7. **Harmonic vibrations**

All the entities are assumed to have the form $f=f^o\sin(\vartheta t-\phi)$, ϑ being the frequency of the excitation, ϕ is the given phase displacement; f^o stands for the amplitude of *f*. Due to the setting being linear the bar's response is also harmonic, with the same frequency and phase displacement, e.g. the axial force has the form: $N=N^o\sin(\vartheta t-\phi)$, etc. Let the end *x*=0 be clamped and the end *x=l* be free and unloaded. The equations of motion link the amplitudes of the internal forces and loads; according to (6.2) we arrive at six variational equations:

$$\int_0^l N\frac{d\bar{u}}{dx}dx-\vartheta^2\int_0^l\mu u\bar{u}dx=\int_0^l p\bar{u}dx \quad \text{for } \bar{u} \text{ such that } \bar{u}(0)=0$$

$$\int_0^l (M_y \frac{d\bar{\beta}}{dx} + T_z\bar{\beta})dx - \vartheta^2 \int_0^l (\tilde{I}_y\beta + I_{yz}\varphi)\bar{\beta}dx = 0 \quad \text{for} \quad \bar{\beta} \quad \text{such that} \quad \bar{\beta}(0) = 0$$

$$\int_0^l T_z \frac{d\bar{w}}{dx} dx - \vartheta^2 \int_0^l (\mu w + \hat{S}_z\theta)\bar{w}dx = \int_0^l q_z\bar{w}dx \quad \text{for} \quad \bar{w} \quad \text{such that} \quad \bar{w}(0) = 0$$

$$\int_0^l (-M_z \frac{d\bar{\varphi}}{dx} + T_y\bar{\varphi})dx - \vartheta^2 \int_0^l (\tilde{I}_z\varphi + I_{yz}\beta)\bar{\varphi}dx = 0 \quad \text{for} \quad \bar{\varphi} \quad \text{such that} \quad \bar{\varphi}(0) = 0 \tag{7.1}$$

$$\int_0^l T_y \frac{d\bar{v}}{dx} dx - \vartheta^2 \int_0^l (\mu v - \hat{S}_y\theta)\bar{v}dx = \int_0^l q_y\bar{v}dx \quad \text{for} \quad \bar{v} \quad \text{such that} \quad \bar{v}(0) = 0$$

$$\int_0^l \left(B\frac{d^2\bar{\theta}}{dx^2} + \mathcal{M}\frac{d\bar{\theta}}{dx} \right) dx - \vartheta^2 \left[\int_0^l (I_o\theta + \hat{S}_z w - \hat{S}_y v)\bar{\theta}dx + \int_0^l \mu_\varpi \frac{d\theta}{dx}\frac{d\bar{\theta}}{dx}dx \right] = \int_0^l m_s\bar{\theta}dx$$

$$\text{for} \quad \bar{\theta} \quad \text{such that} \quad \bar{\theta}(0) = 0, \ \frac{d\bar{\theta}}{dx}(0) = 0$$

The index ‘o’ has been omitted. Now, also the constitutive equations (4.3, 4.4) link the amplitudes. Along with (7.1) these equations are the starting point of the FEM programming.

8. Natural vibrations

8.1. Equations linking the amplitudes

Consider equations linking the amplitudes of harmonic vibrations with the eigenfrequency $\vartheta = \omega$. According to (5.8) the amplitudes of the inertia forces are

$$\Psi_x = -\omega^2\mu u, \quad \Psi_\varpi = -\omega^2\mu_\varpi \frac{d\theta}{dx}, \quad [\Phi_y \Psi_z \Phi_z \Psi_y \Phi_x]^T = -\omega^2 \mathbf{Sq}, \tag{8.1}$$

where now $\{u, \mathbf{q}\}$ is a collection of the amplitudes of the primal unknowns. The equations of motion (6.5) lead to the ordinary differential equations linking the amplitudes:

$$-EA\frac{d^2u}{dx^2} - \omega^2\mu u = 0, \qquad \left(\mathbf{L} - \omega^2\left(\mathbf{S} - \mathbf{C}\right)\right)\mathbf{q} = \mathbf{0} \tag{8.2}$$

where the matrix **S** has been already defined, see (5.9); the operator matrices **C** and **L**, see (6.6), (6.7), involve now the ordinary differential operators d/dx.

8.2. Eigenvibrations of a fork-supported bar

Consider the harmonic vibrations of a fork-supported bar. The amplitudes of displacements are expressed as below

(8.3) $$\left[w\ v\ \theta\right]^T = \left[\hat{w}\ \hat{v}\ \hat{\theta}\right]^T \sin(\alpha_n x), \quad \left[\beta\ \varphi\right]^T = \left[\hat{\beta}\ \hat{\varphi}\right]^T \cos(\alpha_n x), \quad \alpha_n = \frac{n\pi}{l}$$

The bending moments and the bimoment assume the form

(8.4) $$\left[M_y\ M_z\ B\right]^T = \left[\hat{M}_y\ \hat{M}_z\ \hat{B}\right]^T \sin(\alpha_n x), \quad \hat{M}_y = -\alpha_n EJ_y \hat{\beta},\ \hat{M}_z = \alpha_n EJ_z \hat{\varphi},\ \hat{B} = -(\alpha_n)^2 EJ_\varpi \hat{\theta}$$

,

which proves that the fork-supported conditions $N = 0,\ M_y = 0,\ w = 0,\ B = 0,\ M_z = 0,\ v = 0,\ \theta = 0$ are fulfilled identically at both the ends. Let us define the vector: $\hat{\mathbf{q}} = [\hat{\beta}\ \hat{w}\ \hat{\varphi}\ \hat{v}\ \hat{\theta}]^T$ and the matrices

(8.5) $$\mathbf{A}_n = \begin{bmatrix} \frac{n^2\pi^2}{l^2}EJ_y + GA_z & \frac{n\pi}{l}GA_z & GA_{yz} & \frac{n\pi}{l}GA_{yz} & 0 \\ \frac{n\pi}{l}GA_z & \frac{n^2\pi^2}{l^2}GA_z & \frac{n\pi}{l}GA_{yz} & \frac{n^2\pi^2}{l^2}GA_{yz} & 0 \\ GA_{yz} & \frac{n\pi}{l}GA_{yz} & \frac{n^2\pi^2}{l^2}EJ_z + GA_y & \frac{n\pi}{l}GA_y & 0 \\ \frac{n\pi}{l}GA_{yz} & \frac{n^2\pi^2}{l^2}GA_{yz} & \frac{n\pi}{l}GA_y & \frac{n^2\pi^2}{l^2}GA_y & 0 \\ 0 & 0 & 0 & 0 & \frac{n^2\pi^2}{l^2}GJ + \frac{n^4\pi^4}{l^4}EJ_\varpi \end{bmatrix}$$

(8.6) $$\left[\mathbf{C}_n\right]_{ij} = \delta_{i5}\delta_{j5}\frac{n^2\pi^2}{l^2}\mu_\varpi$$

The problem of eigenvibrations has the form: find the pairs $(\hat{\mathbf{q}}, \omega)$ such that

(8.7) $$\left(\mathbf{A}_n - \omega^2\left(\mathbf{S} + \mathbf{C}_n\right)\right)\hat{\mathbf{q}} = \mathbf{0}$$

where $\mathbf{S}$ is given by (5.9). The matrices $\mathbf{A}_n, \mathbf{B}_n = \mathbf{S} + \mathbf{C}_n$ are symmetric and positive definite. The eigenvibrations equations are coupled in general.

Case of mono-symmetric profiles. Due to (6.9) the matrices $\mathbf{A}_n, \mathbf{B}_n = \mathbf{S} + \mathbf{C}_n$ assume the block forms; in particular, the matrix $\mathbf{B}_n$ has the structure as below

$$(8.8)\quad \mathbf{B}_n = \rho_m \begin{bmatrix} J_y & 0 & 0 & 0 & 0 \\ 0 & A & 0 & 0 & 0 \\ 0 & 0 & J_z & 0 & 0 \\ 0 & 0 & 0 & A & z_S A \\ 0 & 0 & 0 & z_S A & \left[J_y + J_z + (z_S)^2 A\right] + \dfrac{n^2\pi^2}{l^2} J_\varpi \end{bmatrix}$$

The problem (8.7) splits up into two problems:

a) bending vibrations in the plane *x-z*: find $\left((\hat{\beta}, \hat{w}/l), \lambda\right)$ such that

$$(8.9)\quad \left(\tilde{\mathbf{A}}_n - \lambda \mathbf{B}\right)\left[\hat{\beta} \;\; \hat{w}/l\right]^{\mathrm{T}} = \left[0\;0\right]^{\mathrm{T}}$$

$$(8.10)\quad \tilde{\mathbf{A}}_n = \begin{bmatrix} \dfrac{n^2\pi^2}{l^2}\dfrac{EJ_y}{GA_z} + 1 & n\pi \\ n\pi & n^2\pi^2 \end{bmatrix} \qquad \mathbf{B} = \begin{bmatrix} \dfrac{E(J_y)^2}{GAA_z l^4} & 0 \\ 0 & \dfrac{EJ_y}{GA_z l^2} \end{bmatrix}$$

The circular frequencies are expressed by $\omega = \sqrt{\lambda}\,\dfrac{1}{l^2}\sqrt{\dfrac{EJ_y}{\rho_m A}}$.

b) lateral (in the *x-y* plane) bending-torsional vibrations : find $\left((\hat{\varphi}, \hat{v}/l, \hat{\theta}), \lambda\right)$ such that

$$(8.11)\quad \left(\breve{\mathbf{A}}_n - \lambda \breve{\mathbf{B}}_n\right)\left[\hat{\varphi} \;\; \hat{v}/l \;\; \hat{\theta}\right]^{\mathrm{T}} = \left[0\;0\;0\right]^{\mathrm{T}}$$

$$(8.12)\quad \breve{\mathbf{A}}_n = \begin{bmatrix} \dfrac{n^2\pi^2}{l^2}\dfrac{EJ_z}{GA_y} + 1 & n\pi & 0 \\ n\pi & n^2\pi^2 & 0 \\ 0 & 0 & \dfrac{n^2\pi^2}{l^2}\dfrac{J}{A_y} + \dfrac{n^4\pi^4}{l^4}\dfrac{EJ_\varpi}{GA_y} \end{bmatrix}$$

$$(8.13)\quad \breve{\mathbf{B}}_n = \begin{bmatrix} \dfrac{EJ_y J_z}{AGA_y l^4} & 0 & 0 \\ 0 & \dfrac{EJ_y}{GA_y l^2} & z_S \dfrac{EJ_y}{GA_y l^3} \\ 0 & z_S \dfrac{EJ_y}{GA_y l^3} & \dfrac{EJ_y}{AGA_y l^4}\left[J_y + J_z + (z_S)^2 A + \dfrac{n^2\pi^2}{l^2} J_\varpi\right] \end{bmatrix}$$

Having λ the circular frequencies are expressed as before.

9. Natural vibrations – case studies

The subject of consideration are natural vibrations of bars: a) of elliptical cross-sections (of bisymmetric cross-sections), and b) the rail 49E1 (of mono-symmetric cross-section). The aim of the research is to check accuracy of the theory of bars discussed in the present paper, governed by the equations of motion (6.2)-(6.4) with the constitutive equations (4.3), (4.4). From the point of view of the classification proposed in [11] this approach can be viewed as the Librescu and Song [12] bar model, since the theory takes into account: transverse shear deformation (in a fashion of Timoshenko's model) as well as the warping due to torsion (in a fashion of Vlasov's model). By neglecting the latter effect one reduces the model to that of Timoshenko, with specific form of the constitutive equations and with special treatment of rotary inertia. On the other hand, neglecting transverse shear deformations reduces the Librescu-Song model to that of Vlasov, and reduces Timoshenko-like model to the Bernoulli-Euler theory. These simplifications will not be discussed in the present paper, as we are interested in considering bars of moderate thickness, not only very thin bars. Thus, we will focus on accuracy of two bar's models: Librescu-Song and Timoshenko-like both based on the assumption (3.1). One of the most interesting questions is the influence of the warping due to torsion on natural vibrations, or, saying in other words, assessing the errors introduced by neglecting this phenomenon in Timoshenko-like models. The natural vibrations are analyzed by the FE approximation. The kinematic fields $\beta, w, \varphi, v, \theta, u$ are interpolated with using four 3rd order polynomials $P_i : [-1,1] \to R$, $i = 0,1,2,3$, or

$$
\begin{aligned}
&\beta(\xi) = q_0 P_0(\xi) + q_1 P_1(\xi) + q_2 P_2(\xi) + q_3 P_3(\xi) \\
&w(\xi) = q_4 P_0(\xi) + q_5 P_1(\xi) + q_6 P_2(\xi) + q_7 P_3(\xi) \\
&\ldots \\
&u(\xi) = q_{20} P_0(\xi) + q_{21} P_1(\xi) + q_{22} P_2(\xi) + q_{23} P_3(\xi)
\end{aligned}
\tag{9.1}
$$

defined on the reference element [–1,+1] as below

$$
\begin{aligned}
&P_0(\xi) = -\frac{1}{8} + \frac{1}{8}\xi + \frac{5}{8}\xi^2 - \frac{5}{8}\xi^3, \quad P_1(\xi) = \frac{5}{8} - \frac{5\sqrt{5}}{8}\xi - \frac{5}{8}\xi^2 + \frac{5\sqrt{5}}{8}\xi^3, \\
&P_2(\xi) = \frac{5}{8} + \frac{5\sqrt{5}}{8}\xi - \frac{5}{8}\xi^2 - \frac{5\sqrt{5}}{8}\xi^3, \quad P_3(\xi) = -\frac{1}{8} - \frac{1}{8}\xi + \frac{5}{8}\xi^2 + \frac{5}{8}\xi^3, \quad \xi \in [-1,1]
\end{aligned}
\tag{9.2}
$$

such that at the nodes of coordinates $\xi_0 = -1, \quad \xi_1 = -\sqrt{5}/5, \quad \xi_2 = \sqrt{5}/5, \quad \xi_3 = 1$ there hold: $P_i(\xi_j) = \delta_{ij}$ for i , j = 0,1,2,3. In this manner a 24-parameter ($q_0, q_1, \ldots, q_{23} \in R$) FE interpolation for the Librescu-Song bar model (1D FEM-LS) is constructed .

All the components of the stiffness matrix and the consistent mass matrix have been computed exactly with using the symbolic program Maple; their expressions are then re-written as C codes with using the command: C(expression, optimized, precision=double). These codes have been then copied to the first author's FEM program computing natural vibrations. In all cases the bar axis has been divided into 100 elements. Accuracy of the FE approximation of the primal unknowns $\beta, w, \varphi, v, \theta, u$ has been checked by numerous static tests, for various boundary conditions; satisfactory results were obtained. Implementation of other FEM interpolation schemes proposed in the literature, as well as a comparative analyses of accuracy are not the aim of the present paper.

The FEM results based on Librescu-Song (1D FEM-LS) and Timoshenko-like models (1D FEM-T are compared with the relevant exact results (1D exact-LS) corresponding to the fork-supported bars, given by Eqs (8.9-8.13). Moreover, the above 1D –models results are confronted with the results found by: a) 3D FEM with using BRIC elements within the SOFISTIK system, b) 1D model of bars with warping, available in the same system (1D FEM-T(W)). The comparisons with 3D solutions have been restricted to the cases of bars clamped at both the ends and to the cantilevers. In fact, the fork support can be interpreted in the 3D modelling in various manners, hence the lack of 3D tests.

9.1. The bar of elliptic cross-section

Our aim is to model the vibrations of a straight prismatic bar whose cross section is the ellipse : $\left(y/a\right)^2 + \left(z/b\right)^2 \le 1$. The geometric and inertia characteristics are

$$
\begin{aligned}
&SC = S, y_S = z_S = 0,\ A = \pi ab,\ \ J_y = \pi\frac{ab^3}{4},\ \ J_z = \pi\frac{ba^3}{4},\ A_{yz} = 0,\ I_{yz} = 0,\ \ \hat{S}_y = 0,\ \hat{S}_z = 0 \\
&\tilde{I}_y = \rho_m J_y,\ \tilde{I}_z = \rho_m J_z,\ \ \mu = \rho_m A,\ \ \mu_\varpi = \rho_m J_\varpi,\ I_y = \tilde{I}_y,\ I_z = \tilde{I}_z,\ \ I_o = \rho_m\left(J_y + J_z\right)
\end{aligned}
\tag{9.3}
$$

Upon solving the torsion problem (2.1) one may compute the torsional and the warping constants:

$$
J = \pi\frac{a^3b^3}{a^2+b^2}\ ,\ J_\varpi = \frac{\pi}{24}\left(\frac{a^2-b^2}{a^2+b^2}\right)^2 a^3b^3 \tag{9.4}
$$

The problems of shear (2.6, 2.8) have been solved numerically by the authors' program (see [11]) and this has paved the way for computing the shear correction factors, see Table 4. It is worth noting here that alternative results have been found by Hutchinson's [9]. They read:

$$
\begin{aligned}
&A_y = k(a/b)A,\ \ A_z = k(b/a)A \\
&k(\xi) = \left(1+\nu\right)^2 \frac{6\xi^2(3\xi^2+1)}{20\xi^4 + 8\xi^2 + \nu(37\xi^4 + 10\xi^2 + 1) + \nu^2(17\xi^4 + 2\xi^2 - 3)}
\end{aligned}
\tag{9.5}
$$

We have checked that the formulae for the effective areas above do not coincide with those determined by the algorithm of Sec. 2, except for the special case of $\nu = 0$.

In all examples the following data have been chosen: E = 2.1E+09 [kg/s^2/cm], ν = 0.3, ρ_m = 0.00785 kg /cm^3. We fix attention on the case of b/a=3, see Fig.1, where the FE mesh of the cross-section domain used for the alternative computing of the characteristics (9.3-9.4) is shown. The analysis will concern the bar of length l = 900 cm, and the transverse dimensions: $2a$=20 cm, $2b$=60 cm. The assumed cross-section has huge dimensions, but it does not matter, since the results concerning the frequency $f = \omega/(2\pi)$ [Hz] can be easy rescaled, if all the dimensions are changed with the same proportionality coefficient; note that the solution λ to the problems (8.9, 8.11) is independent of this coefficient. The FE triangulation of the ellipse results in approximating the contour by a zig-zag line, which has resulted in appearing differences between the analytical and numerical results concerning the characteristics A, J_y, J_z, J, J_ω, see Table 1. Moreover, the effective areas A_y, A_z computed by Hutchinson's formulae (9.5) differ from those predicted by Gruttmann and Wagner's algorithm (Sec.2).

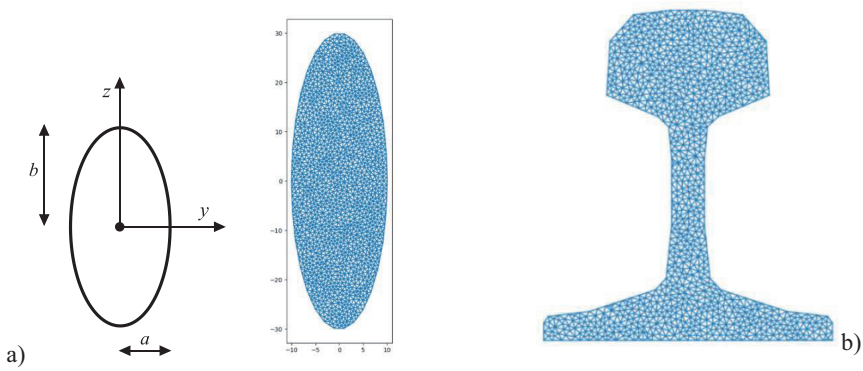

Fig. 1. Elliptic cross- section; the FEM mesh used for a = 10 [cm], b = 3a; (a). The rail 49E1 cross-section- the FEM mesh used; the interpolation of the rounded edges of the rail does not perfectly reproduce the sectional shape (b)

Table 1. Geometric characteristics of the elliptical cross section of Fig.1a. The FE approximants of the effective areas have been found with using the authors' program implementing the algorithm [8].

	A cm^2	J_y cm^4	J_z cm^4	J cm^4	J_ω cm^6	A_y cm^2	A_z cm^2
Analytical results	942	211950	23550	84780	2.26E+6	844	877
Numerical results	925	208987	23219	83669	2.21E+06	617	836

Due to bisymmetry of the cross-section, under the condition of the boundary conditions being also bisymmetric, the problem of natural vibrations splits up into three independent problems: bending in *x-z* plane, bending in *x-y* plane and torsion.

The present section concerns free vibrations for various support conditions, with using: the 1D FEM-LS. The results are compared with exact results within the same bar model. The first seven natural frequencies $f = \omega/(2\pi)$ [Hz] are set up in Table 2. The FE program computes these frequencies with good accuracy; small errors are visible in the way the higher frequencies of torsional vibrations are predicted. In Table 3 the natural frequencies of the bar clamped at both ends and of the cantilever are set up. These results are not compared here with analytical predictions.

Table 2. The natural frequencies (the units: [Hz]) of the vertical, horizontal and torsional vibrations of the fork-supported bar of elliptic cross-section, computed by the first author's FE program (in C++) implementing the Librescu-Song bar model and- by the analytical formulae (8.9-8.13) derived from the same bar model.

Vertical		Horizontal		Torsional	
1D FEM -LS	1D exact-LS	1D FEM -LS	1D exact-LS	1D FEM -LS	1D exact-LS
14.9	14.9	5.0	5.0	107.0	107.0
58.7	58.7	19.9	19.9	214.2	214.2
129.0	129.0	44.7	44.7	321.9	321.9
222.1	222.1	79.0	79.0	429	430
334.5	334.5	122.6	122.6	536	540
462.3	462.3	175.2	175.2	654	650
602.4	602.4	236.4	236.4	757	762

Table 3. The first ten natural frequencies of the bar of elliptic cross-section: clamped at both ends (the first row), the cantilever (the second row), predicted by the FE program implementing the Librescu and Song model.

Natural frequencies[Hz]	f_1	f_2	f_3	f_4	f_5	f_6	f_7	f_8	f_9	f_{10}
The bar clamped at both the ends	11.3	31.0	33.3	60.4	89.3	99.2	106.0	147.1	169.4	203.5
The cantilever	1.78	5.33	11.13	31.05	32.90	53.48	60.56	90.07	99.48	143.67

9.2. The rail 49E1

The subject of the dynamic analysis will be rails of the profile 49E1 of various lengths. The FE mesh for the profile has been constructed by using the dimensions given in: https://rails.arcelormittal.com/lang/pl/pages/168-49e1-s49 ; see Fig. 1b. The rail's cross section is mono-symmetric; its geometric characteristics are set up in Table 4, the center of gravity lies at the distance h_O from the base of the rail; it does not coincide with the center of shear S.

Table 4. The rail 49E1 characteristics computed by SOFISTIK (first row) and calculated by the present author's program upon introducing the contour of the shape shown in Fig.1b. (second row)

Rail 49E1	h_O cm	A cm^2	J_y cm^4	J_z cm^4	y_S cm	z_S cm	k_z	k_y	k_{zy}	J cm^4	I_ω cm^6
SOFISTIK	7.26	62.68	1789.0	313.10	0.0	-2.45	0.363	0.601	0.0	175.10	-
Authors' program	7.27	62.31	1778.14	306.11	0.0	-2.45	0.367	0.601	0.0	176.68	7946.7

The fork-supported rails

The natural vibrations split into: flexural vibrations in the *x-z* plane (vertical vibrations), and the coupled: flexural horizontal – torsional vibrations. The vibrations of the rails (49E1) of lengths: 1m, 2m, 4m, fork-supported, have been examined by four methods: 1D FEM-T (Table 5), 1D FEM-LS (Table 6), 1D exact-LS (Table 7), 1D FEM-T(W) (Table 8). We note that all the methods used deliver accurate results concerning vibrations in vertical direction. The accuracy increases along with slenderness.

Table 5. The natural frequencies ([Hz]) of the vertical and horizontal-torsional vibrations of the fork-supported rail 49E1 computed by the FE model for the Timoshenko-like theory (1D FEM-T)

l=1.0[m]		*l*=2.0[m]		*l*=4.0[m]	
Vertical	Horizontal-torsional	Vertical	Horizontal-torsional	Vertical	Horizontal-torsional
392.11	179.25	105.54	45.25	26.93	11.34
1269.20	691.46	392.11	179.25	105.54	45.25
2289.39	1474.05	797.87	397.11	229.91	101.40
3331.88	2455.00	1269.2	691.46	392.11	179.26
4367.25	3571.99	1772.47	1053.53	583.91	278.12

Table 6. The natural frequencies ([Hz]) of the vertical and horizontal-torsional vibrations fork-supported rail 49E1 computed by the FE model for the Librescu and Song theory (1D FEM-LS)

l=1.0[m]		*l*=2.0[m]		*l*=4.0[m]	
Vertical	Horizontal-torsional	Vertical	Horizontal-torsional	Vertical	Horizontal-torsional
392.44	175.15	105.56	44.72	26.93	11.24
1272.1	472.89	392.44	175.15	105.56	44.72
2297.07	631.77	799.13	234.16	230.01	99.76
3345.36	1004.90	1272.1	379.00	392.44	116.82
4386.84	1147.12	1777.57	472.94	584.61	175.15

Table 7. The natural frequencies ([Hz]) of the vertical and horizontal-torsional vibrations fork-supported rail 49E1 computed by the exact formulae (8.9-8.13), or (1D exact-LS)

l=1.0[m]		*l*=2.0[m]		*l*=4.0[m]	
Vertical	Horizontal-torsional	Vertical	Horizontal-torsional	Vertical	Horizontal-torsional
392.30	175.38	105.51	44.70	26.92	11.23
1271.81	498.51	392.30	175.38	105.51	44.70
2296.72	653.94	798.91	237.47	229.93	99.77
3345.01	1172.92	1271.81	382.62	392.30	117.24
4386.51	1347.64	1777.24	498.51	583.43	175.38

Table 8. The natural frequencies ([Hz])of the vertical and horizontal-torsional vibrations fork-supported rail 49E1 computed by SOFISTIK – FEM for Timoshenko model with warping (1D FEM-T(W))

l=1.0[m]		*l*=2.0[m]		*l*=4.0[m]	
Vertical	Horizontal-torsional	Vertical	Horizontal-torsional	Vertical	Horizontal-torsional
392.24	176.57	105.56	45.10	26.94	11.33
1270.26	470.48	392.32	176.61	105.58	45.11
2292.42	635.56	798.69	232.56	230.10	100.65
3337.87	1007.63	1271.21	381.98	392.67	115.98
4377.23	1154.42	1776.32	470.49	585.14	176.78

To make the results set up in Tables 5-8 better visible the natural frequencies concerning the vertical vibrations (index V) and the lateral-torsional vibrations (index H) computed by the 1D FE methods

based on the theories by: Timoshenko (index: T), Librescu-Song (index L) and the Timoshenko-like theory being the basis for the SOFISTIK FEM model with warping (index S) will be referred to the exact results based on the Librescu-Song theory (index E). The Figures 2-7 show the relative errors of assessing the first five natural frequencies f. The following notation of the methods used for computing the frequencies is adopted:

f_{VT}, f_{HT} : the FE model for the Timoshenko-like theory,

f_{VL}, f_{HL} : the FE model for the Librescu and Song theory,

f_{VS}, f_{HS} : SOFISTIK – FEM for Timoshenko-like model with warping,

f_{VE}, f_{HE} : the exact formulae (8.9-8.13) according to the Librescu-Song theory.

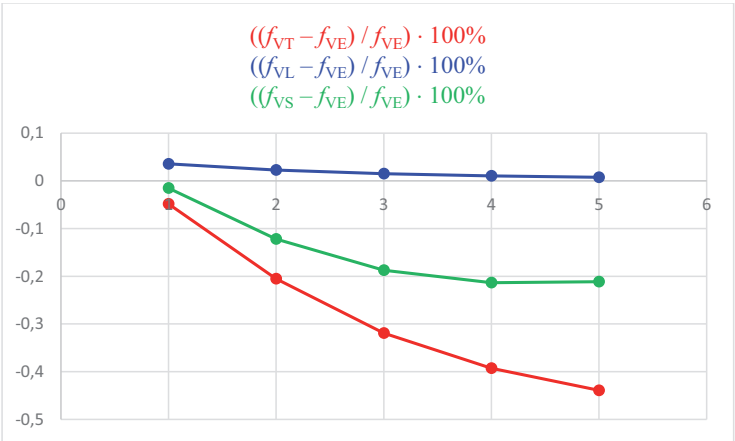

Fig. 2. The rail of length $l = 1.0$ [m]. Relative error of assessing the first five natural frequencies of vertical vibrations of the fork-supported rail 49E1, computed by 1D FEM-T, 1D FEM-LS, and SOFISTIK 1D FEM-T(W) models.

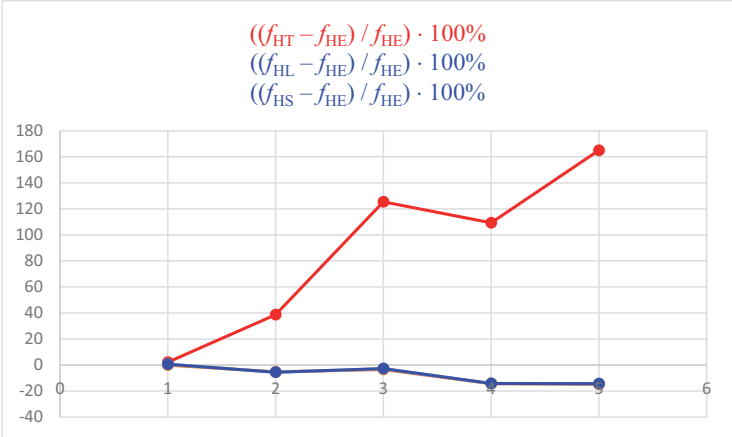

Fig. 3. The rail of length $l = 1.0$ [m]. Relative error of assessing the first five natural frequencies of horizontal-torsional vibrations of the fork-supported rail 49E1, computed by 1D FEM-T, 1D FEM-LS, and SOFISTIK 1D FEM-T(W) models.

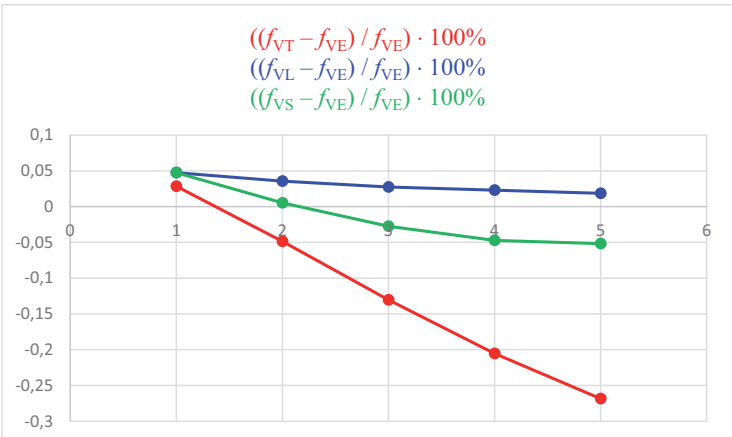

Fig. 4. The rail of length $l = 2.0$ [m]. Relative error of assessing the first five natural frequencies of vertical vibrations of the fork-supported rail 49E1 computed by 1D FEM-T, 1D FEM-LS, and SOFISTIK 1D FEM-T(W) models.

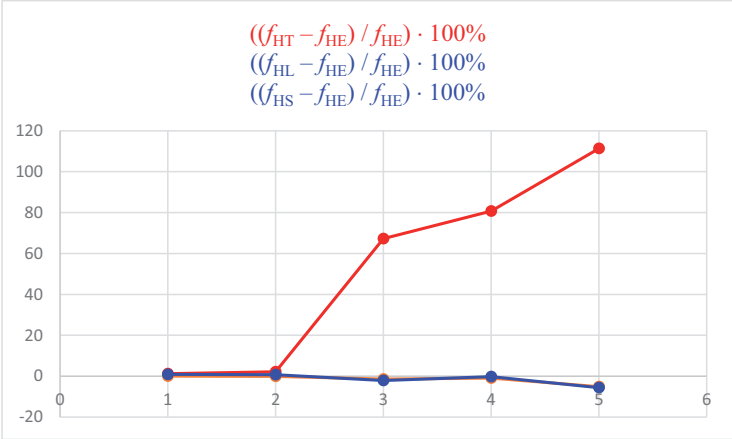

Fig. 5. The rail of length $l = 2.0$ [m]. Relative error of assessing the first five natural frequencies of horizontal-torsional vibrations of the fork-supported rail 49E1 computed by 1D FEM-T, 1D FEM-LS, and SOFISTIK 1D FEM-T(W) models.

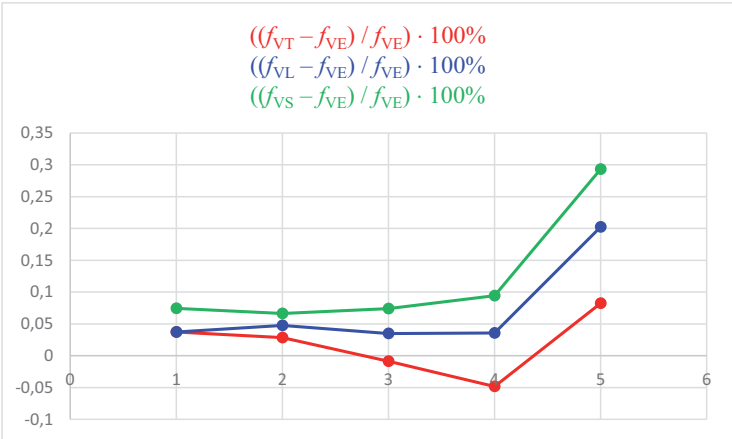

Fig. 6. The rail of length $l = 4.0$ [m]. Relative error of assessing natural frequencies of vertical vibrations of the fork-supported rail 49E1 computed by 1D FEM-T, 1D FEM-LS, and SOFISTIK 1D FEM-T(W) models.

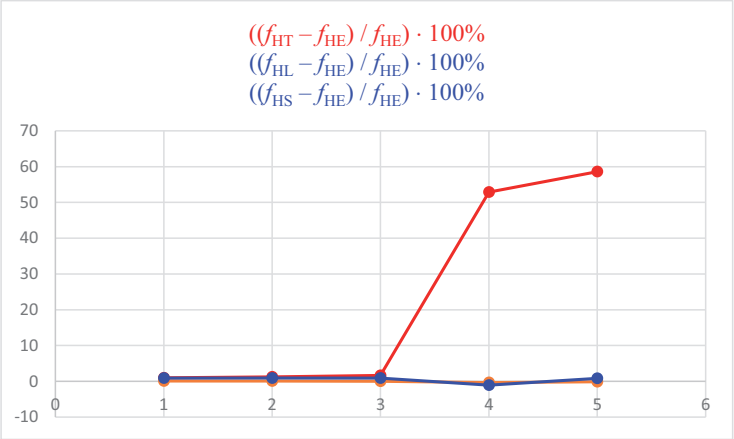

Fig. 7. The rail of length $l = 4.0$ [m]. Relative error of assessing natural frequencies of horizontal-torsional vibrations of the fork-supported rail 49E1 computed by 1D FEM-T, 1D FEM-LS, and SOFISTIK 1D FEM-T(W) models.

The Timoshenko model without warping predicts correctly only selected horizontal-torsional natural frequencies, while the accuracy decays if the thickness-to-span ratio increases. By incorporating warping effects due to torsion the description of these vibrations is improving, which stresses the significance of the Librescu-Song-like model proposed in the present paper. It is worth noting that the model of the torsional warping in SOFISTIK also delivers accurate results, see Table 8 and Figs 2-7.

Other boundary conditions

The vibrations of bars of lengths 1m, 2m, 4m, clamped at both ends have been examined by the methods : 1D FEM-T, 1D FEM-LS and 3D FEM (with using SOFISTIK 3D BRIC non-conforming elements) see Tables 9, 10. Let us note that the model (1D FEM-T) omits some natural vibration eigenmodes, even if the bar is very thin (case of l=4m), while the Librescu-Song model delivers good results, uniformly.

The vibrations of the same bars, but clamped at one end (the cantilevers) are correctly predicted by the Librescu-Song model, while Timoshenko's model omits some eigenvibration modes, even if l=4m, see Tables 11,12.

Table 9. Natural frequencies ([Hz]) of the bars clamped at both ends predicted by: the first author's FE code implementing the Timoshenko model, and by SOFISTIK with using non-conforming 3D BRIC elements. The signs: "-" mean that the relevant frequency could not be assigned to the 3D prediction

l=1.0[m]		*l*=2.0[m]		*l*=4.0[m]	
1D FEM-T	3D FEM	1D FEM-T	3D FEM	1D FEM-T	3D FEM
390.44	345.55	101.54	100.37	25.65	25.53
-	523.40	219.15	220.56	59.60	59.59
689.03	689.21	275.10	259.45	70.39	69.78
-	778.52	527.52	502.44	-	115.79
-	1201.21	538.87	544.30	137.17	136.15
-	1222.93	849.25	787.77	158.36	158.36
1492.24	1493.19	940.93	953.46	225.08	216.11
2425.03	2427.34	-	1115.70	296.88	297.03
3403.18	3407.75	1231.2	1296.09	460.81	467.00
4405.14	4413.01	-	1482.84	660.08	661.20

Table 10. Natural frequencies ([Hz]) of the bars clamped at both ends predicted by: the first author's FE code implementing the Librescu-Song model, and by SOFISTIK with using non-conforming 3D BRIC elements

l=1.0[m]		*l*=2.0[m]		*l*=4.0[m]	
1D FEM-LS	3D FEM	1D FEM-LS	3D FEM	1D FEM-LS	3D FEM
344.03	345.55	98.70	100.37	25.31	25.53
522.77	523.40	219.27	220.56	59.59	59.59
690.59	689.21	261.64	259.45	69.18	69.78
775.89	778.52	482.72	502.44	116.25	115.79
1191.46	1201.21	539.63	544.30	135.04	136.15
1212.75	1222.93	749.92	787.77	158.37	158.36
1497.00	1493.19	942.87	953.46	214.55	216.11
2433.68	2427.34	1057.65	1115.70	297.02	297.03
3416.38	3407.75	1293.05	1296.09	466.92	467.00
4423.30	4413.01	1496.65	1482.84	660.90	661.20

Table 11. Natural frequencies ([Hz]) of the cantilever bars predicted by: the first author's FE code implementing the Timoshenko model, and by SOFISTIK with using non-conforming 3D BRIC elements. The signs: "-" mean that the relevant frequency could not be assigned to the 3D prediction

l=1.0[m]		*l*=2.0[m]		*l*=4.0[m]	
1D FEM-T	3D FEM	1D FEM-T	3D FEM	1D FEM-T	3D FEM
64.32	64.14	16.15	16.15	4.04	4.04
146.99	147.66	38.16	38.23	9.64	9.64
-	253.91	100.32	98.95	25.28	25.24
389.22	382.18	-	122.85	59.21	59.28
733.02	741.74	222.34	223.09	-	59.43
-	761.15	276.93	269.98	70.53	70.23
1035.86	965.55	-	366.11	137.48	136.13
-	1296.09	565.69	568.77	160.91	161.17
-	1436.63	-	617.80	-	178.05
1660.38	1685.67	991.99	999.23	225.71	222.12

Table 12. Natural frequencies of the cantilever bars predicted by: the first author's FE code implementing the Librescu-Song model, and by SOFISTIK with using non-conforming 3D BRIC elements

l=1.0[m]		l=2.0[m]		l=4.0[m]	
1D FEM-LS	3D FEM	1D FEM-LS	3D FEM	1D FEM-LS	3D FEM
63.34	64.14	15.99	16.15	4.01	4.04
146.97	147.66	38.15	38.23	9.63	9.64
232.26	253.91	97.30	98.95	24.99	25.24
378.56	382.18	118.66	122.85	58.40	59.28
695.25	741.74	222.39	223.09	59.19	59.43
734.16	761.15	264.72	269.98	69.52	70.23
935.76	965.55	357.83	366.11	134.56	136.13
1230.02	1296.09	566.21	568.77	160.90	161.17
1469.13	1436.63	611.03	617.80	175.44	178.05
1664.46	1685.67	993.59	999.23	219.56	222.12

Conclusions

The paper proves that the free vibrations of bars of mono-symmetric profiles cannot be correctly described by the Timoshenko-like theories, even if all the inertia terms are consistently kept. To predict the natural frequencies correctly one should introduce the warping terms due to torsion into the kinematic assumptions, as already Vlasov did to model deformations of thin-walled bars. Here, however, this concept is extended to the bars of solid compact cross-sections, like rails. The 1D modelling has to be preceded by constructing solutions to the 2D scalar elliptic problems describing warping due to torsion and transverse shear correction. The dynamic analysis involves all the inertia terms induced by the enhanced kinematics thus assuring high accuracy of computing the natural frequencies of coupled bending-torsional vibrations of relatively thick bars. This extension paves the way for the dynamic analysis of systems of bars, like railway tracks.

Acknowledgements

The work was conducted as part of the project " Innovative solutions of people and the environment protection against rail traffic noise ", co-financed by the European Regional Development Fund within the Operational Programme Smart Growth 2014-2020 and has been also partly supported by the grant of the Scientific Council of the Discipline of Civil Engineering and Transport of the Warsaw University of Technology within the Research Grant program for the academic year 2020/2021.

References

[1] C. Adam, "Forced vibrations of elastic bending-torsion coupled beams", *Journal of Sound and Vibration* 221, pp. 273–287, 1999. https://doi.org/10.1006/jsvi.1998.2005

[2] J.R. Banerjee, S. Guo, W.P. Howson, "Exact dynamic stiffness matrix of a bending-torsion coupled beam including warping", *Computers and Structures* 59, pp. 613–621,1996. https://doi.org/10.1016/0045-7949(95)00307-X
[3] A. N. Bercin, M. Tanaka, "Coupled flexural-torsional vibrations of Timoshenko beams", *Journal of Sound and Vibration* 207, pp. 47–59, 1997. https://doi.org/10.1006/jsvi.1997.1110
[4] A. Burlon, G. Failla, F. Arena, "Coupled bending–torsional frequency response of beams with attachments: exact solutions including warping effects", *Acta Mechanica* 229, pp. 2445–2475, 2018. https://doi.org/10.1007/s00707-017-2078-y
[5] S. B. Dong, S. Çarbaş, E. Taciroglu, "On principal shear axes for correction factors in Timoshenko beam theory". *International Journal of Solids and Structures* 50, pp. 1681–1688, 2013; Corrigendum: ibidem 62: 274, 2015. http://dx.doi.org/10.1016/j.ijsolstr.2013.01.034
[6] R. El Fatmi, "Non-uniform warping including the effects of torsion and shear forces. Part I: a general beam theory", *International Journal of Solids and Structures* 44, pp. 5912–5929, 2007. https://doi.org/10.1016/j.ijsolstr.2007.02.006
[7] A. Genoese, A. Genoese, A. Bilotta, G. Garcea, "A mixed beam model with non-uniform warpings derived from the Saint Venànt rod", *Computers and Structures* 121, pp. 87–98, 2013. https://doi.org/10.1016/j.compstruc.2013.03.017
[8] F. Gruttmann, W. Wagner, "Shear correction factors in Timoshenko's beam theory for arbitrary shaped cross-sections", *Computational Mechanics* 27, pp. 199–207, 2001. https://doi.org/10.1007/s004660100239
[9] J. R. Hutchinson, "Shear coefficients for Timoshenko beam theory", *Journal of Applied Mechanics*, *ASME*, 68, pp. 87–92, 2001. https://doi.org/10.1115/1.1349417
[10] D. Kostovasilis , D.J. Thompson , M.F.M. Hussein,"A semi-analytical beam model for the vibration of railway tracks", *Journal of Sound and Vibration*, 393, pp. 321–337, 2017. https://doi.org/10.1016/j.jsv.2016.12.033
[11] T. Lewiński, S. Czarnecki, "On incorporating warping effects due to transverse shear and torsion into the theories of straight elastic bars", *Acta Mechanica*, 232, pp. 247-282, 2021. https://doi.org/10.1007/s00707-020-02849-7
[12] L. Librescu, O. Song, "*Thin-Walled Composite Beams. Theory and Application*". Springer, Dordrecht 2006. ISBN 978-1-4020-4203-4
[13] Technishe Lieferbedingungen DBS, "Schienenstegdämpfer (SSD) 918 290, Oberbautechnische und akustische Anforderungen", Deutsche Bahn-Standard 2017

Drgania prętów z uwzględnieniem odkształceń postaciowych oraz spaczenia przy skręcaniu

Słowa kluczowe: teoria prętów, drgania giętno-skrętne, teoria Timoshenki, teoria Librescu i Song

Streszczenie :

Przedmiotem pracy są drgania giętno-skrętne prętów prostych pryzmatycznych, z jednorodnego izotropowego materiału liniowo sprężystego. Jednym z celów pracy jest analiza drgań szyn kolejowych o przekrojach monosymetrycznych z uwzględnieniem spaczenia towarzyszącego deformacji skrętnej, z uwzględnieniem odkształceń postaciowych poprzecznych metodą Timoshenki. Wykazano przydatność modelu Librescu i Song w ujęciu własnym autorów (Acta Mechanica, vol. 232, pp. 247-282, 2021) z członami bezwładnościowymi dokładnie korespondującymi z przyjętą hipotezą kinematyczną. Opracowano program MES tego modelu pręta.

Praca wskazuje na istotną usterkę modelu Timoshenki w opisie drgań własnych szyn kolejowych. O ile drgania giętne w płaszczyźnie symetrii szyny są opisywane poprawnie, to drgania sprzężone: boczne giętne i skrętne są opisywane błędnie; teoria Timoshenki pomija istotne postacie drgań własnych; postacie te dobrze wychwytuje, w sumie niewiele bardziej złożony, model Librescu i Song, a tym bardziej – analiza 3D - przeprowadzona w pracy z pomocą programu SOFISTIK z użyciem niedostosowanych elementów BRIC. Opracowany program MES modelu Librescu i Song jest gotowy do stosowania w analizie drgań torów kolejowych.

Received: 25.10.2020, Revised: 09.02.2021